Physics of the Earth and Planetary Interiors 212–213 (2012) 106–113

Contents lists available at SciVerse ScienceDirect

Physics of the Earth and Planetary Interiors

journal homepage: www.elsevier.com/locate/pepi

Global paleo-lithospheric models for geodynamical analysis of plate reconstructions

L. Quevedo [a,*], G. Morra [a,b], R.D. Müller [a]

[a] EarthByte Group, School of Geosciences, University of Sydney, New South Wales, Australia
[b] School of Earth and Environmental Sciences, Seoul National University, Seoul, South Korea

ARTICLE INFO

Article history:
Received 28 November 2011
Received in revised form 7 September 2012
Accepted 26 September 2012
Available online 23 October 2012
Edited by Mark Jellinek

Keywords:
Subduction history models
Plate reconstructions
Slab dip
Stokes flow
Global geodynamics

ABSTRACT

We present a general framework to generate time-dependent global subduction history models from kinematic plate reconstructions and explore their associated coupled plate–mantle dynamic behaviour. Slabs are constructed by advecting material into the mantle by prescribing its radial velocity and following the absolute tangential motion of the subducting plate. A simple geodynamic scenario where plates and slabs define isopycnic and isoviscous regions in an homogeneous or layered mantle was explored using the boundary element method-based software BEMEarth. The resulting dynamic behaviour was used to predict the absolute plate motion directions for the present day and a particular mid-cretaceous (125 Ma) kinematic model. We show how the methodology can be used to compare and revise kinematic reconstructions based on their effect on the balance of plate driving forces and the resulting Euler poles of subducting plates. As an example we compare the Farallon plate dynamics at 125 Ma in a global model with two reconstructions in the context of the evolution of the Western North American Cordillera. Our results suggest a method to identify episodes of absolute plate motions that are inconsistent with the expected plate dynamics.

1. Introduction

Plate tectonic reconstructions are an essential constraint for understanding the structure and evolution of the mantle that led to a key paradigm of geodynamics: subduction history directly controls fast seismic velocity anomalies within the Earth. In addition, slabs descending into the mantle are associated with geoid highs and may be related to long-lived dynamics of large-scale upwellings associated with low seismic velocity anomalies (Anderson, 1982; Chase and Sprowl, 1983; Chase, 1979; Richards and Engebretson, 1992). The study of mantle flow through geodynamic models relies on plate reconstructions to set up initial density, viscosity and temperature conditions, and to control their evolution through boundary and kinematic constraints. Time-dependent mantle convection models have been constructed by "steering" the lithosphere towards convergent margins (Bunge et al., 1998), imposing vertical sinking velocities to cold material located at subduction zones from plate reconstructions (Ricard et al., 1993; Lithgow-Bertelloni and Richards, 1998), and more recently *assimilating* data to refine the structure of the mantle inferred from backward-advecting present day mantle tomography (Bunge et al., 2003).

By the same token, geodynamic modelling can actively provide independent constraints to tectonic reconstructions. Present day tomography has been compared with the output of forward models to refine our understanding of the past absolute motions of the plates (Shephard et al., 2012), suggesting that simple self-consistent models that predict kinematics *ab initio* could also contribute to bridge the gap between our increasingly complex tectonic reconstructions and our lack of knowledge about the history of global mantle flow. Pull forces associated with subducting slabs are considered to be the main driver of large-scale mantle flow and plate tectonics (Billen, 2008). Since the main factors determining such forces are the geometry and the density contrast of the slab, and since the latter is primarily controlled by the thermal history of oceanic lithosphere, the first-order features of mantle flow as well as absolute plate motions can be inferred from *subduction history models* (Steinberger, 2000). These kind of models have been successful in predicting plate motions consistent with reconstructions (Conrad and Lithgow-Bertelloni, 2002; Morra et al., 2012), true polar wander evolution (Steinberger and Torsvik, 2010), plate driving forces (Conrad and Lithgow-Bertelloni, 2004), dynamic topography and marine inundation patterns of continents (Gurnis, 1993; Lithgow-Bertelloni and Gurnis, 1997; Lithgow-Bertelloni and Richards, 1995). By comparing not only the resulting mantle structure, but also the predicted kinematics with observations, we might be able to reduce uncertainties in our reconstructions.

In this paper we present an original method to produce present and paleo-models for the global shape of lithosphere given in terms of 3D boundary element surface meshes, by defining plate boundaries and advecting material into the mantle following

* Corresponding author.
E-mail address: leonardo.quevedo@sydney.edu.au (L. Quevedo).

0031-9201/$ - see front matter © 2012 Elsevier B.V. All rights reserved.
http://dx.doi.org/10.1016/j.pepi.2012.09.007

reconstructed plate and subduction zone geometries and velocities. At the present day, models with a prescribed sinking rate can be directly correlated with regions of anomalous fast seismic velocity in global tomography. Boundary element based geodynamic models initialised by these meshes are able to fit the motion of subducting plates at the present day and are used to predict those at the mid-cretaceous, suggesting a method to revise kinematic reconstructions based on their contrasts with their associated dynamics.

2. Modelling approach

The success of previous self-consistent subduction history models in reproducing global plate motion trends (Lithgow-Bertelloni and Richards, 1998) lead us to propose them as a mean to identify where mantle dynamics is not consistent with kinematic reconstructions in the hope of improving them. To overcome the computational limitations associated with multi-scale global tectonic simulations (Becker, 2010), our models are based on the assumption that the coupled mantle–lithosphere dynamics can be approximated by a multiphase flow of regions with homogeneous density and viscosity, disregarding chemical and rheological inhomogeneities (Ribe, 2010; Morra et al., 2012). The global mantle flow is assumed to be controlled by the buoyancy contrasts between the phases (mantle, lithosphere, air and core), the viscous drag contributions to plate motions and the viscous resistance to stretching and bending.

We follow a top-down approach (Lithgow-Bertelloni and Richards, 1995) where subducted slabs represent the leading contribution to internal density heterogeneities that drive tectonics. Plate motions and mantle flow are calculated using the boundary element solution of Stokes multiphase flow as implemented by the BEMEarth code, focusing on the contribution of the main slabs to circulation without considering thermal effects that could affect slab density or viscosity. Such multiphase flow dynamics results in very coherent plate motion resembling standard laboratory experiments on viscous slab subduction (Bellahsen et al., 2005), and is consistent with the classical interpretation of slab pull as the predominant driver of tectonics (Forsyth and Uyeda, 1975; Lithgow-Bertelloni and Richards, 1998). Both slab pull and suction are simultaneously described, leading to the observed velocity asymmetry between subducting and overriding plates. Slabs in our models act effectively as barriers restricting the influence of mantle flow induced by pull on the dynamic of the overriding plates (see Fig. 1).

Recent numerical studies have shown that more than 90% of energy dissipation in the coupled mantle–lithosphere system occurs through creeping mantle flow, implying a direct relation to sinking velocity resulting from the balance between slab pull and mantle drag (Capitanio et al., 2007, 2009; Stadler et al., 2010). Sinking velocity and in general the motion of a plate in subduction models is only mildly influenced by trench motion and plate strength, and is mainly controlled by their overall geometry (Funiciello et al., 2003; Capitanio et al., 2007; Stegman et al., 2006; Morra et al., 2012) which can be inferred from tectonic paleo-reconstructions. The feedback between geometry and dynamics of plate motion suggests that the correlation between past plate geometries and motion can be explored using simple geodynamic models based on the subduction history. Accordingly, we have estimated the overall shape of lithospheric plates and slabs, based on the geometrical and kinematic information of paleo-kinematic reconstructions from which subduction history is inferred.

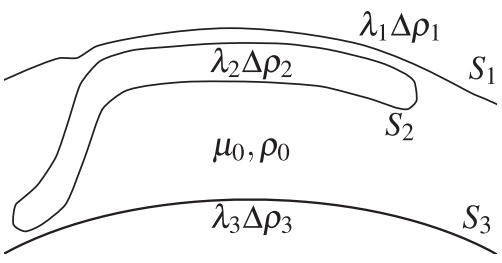

Fig. 1. Schematic diagram of the subducting plate setup as a multiphase flow bounded by the free surfaces S_i. S_1 represents the surface of the Earth, S_2 the surface of the subducting plate, and S_3 the core–mantle boundary.

Although the feedback between orogeny and interplate friction has been previously considered as a factor contributing to the balance of plate driving forces (Iaffaldano et al., 2006), mountain belt growth at convergent margins has been also linked to thickness heterogeneities in the plates involved (Capitanio et al., 2011). As the relative importance of interplate friction in the general context of self-consistent global models remains unclear, the scarcity and uncertainty of paleo-elevation records does not justify a global estimation of the topographical load on paleo plates during the Mesozoic and Cenozoic to be used as an agent of plate motion. We assume frictionless contacts and consider that shear force gradients from the ensuing plate thickness variations are more important for the underlying subduction dynamics.

Since values of mantle viscosity within observational constraints (Mitrovica, 1996) still allow direct fitting of plate speeds using the known inverse relation between speed and viscosity (Lithgow-Bertelloni and Richards, 1998), we choose to focus on the predicted *directions* instead of the *magnitudes* of plate motion. To this aim, we calculate the best fitting Euler pole to the surface flow of each volume representing a plate and compare the deviations of the resulting rigid velocity field with the kinematic reconstruction, to characterise how compatible the plate motions are with the modelled slab pull.

2.1. Model setup

The relevant physical parameters for the multiphase model are the constant viscosity (density) μ_0 (ρ_0) of the mantle, the relative viscosity (differential density) contrast $\lambda_i = \mu_i/\mu_0$ ($\Delta\rho_i = \rho_i - \rho_0$) at each of the surfaces (see Fig. 1), and their shape. In contrast to previous work on global mantle flow (Conrad and Lithgow-Bertelloni, 2002, 2004), pull and suction forces are a direct consequence of the geometry of subducting slabs and are not imposed at the boundaries of the plates. Reference values for mantle density ($\rho_0 = 3300\ \mathrm{kg\ m^{-3}}$) and slab–mantle density contrasts ($\Delta\rho = 30\ \mathrm{kg\ m^{-3}}$) are chosen to be consistent with previous bounds for young lithosphere (Cloos, 1993). The reference viscosity ($\mu_0 = 10^{21}$ Pa s) is chosen in accordance to glacial isostatic adjustment estimates (Mitrovica, 1996), and the slab–mantle viscosity contrast ($\lambda_{SM} = 10$—200) is within the range of values usually selected in the literature for which two or three orders of magnitude ratio are to be found (Funiciello et al., 2003; Bellahsen et al., 2005; Schellart, 2005; Gerya et al., 2008; Capitanio et al., 2009; Morra et al., 2012). We explore upper–lower mantle viscosity contrast in the ($\lambda_{UL} = 1$—100) range. A summary of the physical parameters is presented in Table 1.

2.2. Numerical method

The steady low Reynolds number flow governing our approximation of plate tectonics and mantle dynamics is described by the Stokes equation $\nabla \cdot \boldsymbol{\sigma} + \rho\mathbf{b} = 0$, where σ_{ij} is the full stress tensor and $\mathbf{b}$ represents the (buoyancy) body forces. Using the Green's function method, this problem can be solved as an integral

Table 1
Basic model parameters.

Density		
Mantle	ρ_M	3300 kg m^{-3}
Lithosphere	$\Delta\rho$	30 kg m^{-3}
Viscosity		
Upper mantle	μ_0	10^{21} Pa s
Lower mantle	μ_{LM}	$(1, 50, 100, 200)\,\mu_0$
Lithosphere	μ	$(10, 50, 100, 200)\,\mu_0$
Gravity	g	9.81 m s^{-2}

equation defined only on the interfaces between isoviscous and isopycnic regions that are to define the plates, core and Earth surface boundaries. Given the fundamental solutions for the velocity and traction fields G and T known as the *Stokeslet* and the *Stresslet* solutions (see Pozrikidis, 1992, Section 3), the velocity field $\mathbf{v}(\mathbf{x})$ of the multiphase flow can be found at the phase boundaries $\mathbf{x} \in S_i$ by solving

$$\frac{1+\lambda_i}{2}\mathbf{v}(\mathbf{x}) - \sum_j^N \frac{1-\lambda_j}{8\pi}\int_{S_j}^{PV} \mathbf{n}\cdot\mathsf{T}\cdot\mathbf{v}\,dS = -\frac{1}{8\pi\mu_0}\sum_j^N \int_{S_j} \mathsf{G}\cdot\Delta\mathbf{f}\,dS, \tag{1}$$

where $\Delta\mathbf{f} = \Delta\rho(\mathbf{b}\cdot\mathbf{x})\mathbf{n}$ is the stress jump induced by differential buoyancy between regions, $\mathbf{n}$ is the normal to the surface on the point $\mathbf{x}$, and *PV* denotes the principal value of the integral. This equation can be perturbed beyond homogeneous background viscosity to include mantle layering, by following a procedure described in Morra et al. (2012, Section A). We use the fast multipole accelerated boundary element method to solve the linear system resulting from the discretisation of the Fredholm integral (1) by means of the BEMEarth code (Morra et al., 2007, 2009, 2010, 2012; Quevedo et al., 2010, 2012). Once the values of the velocity are known on the nodes defining each surface, BEMEarth uses second order Runge–Kutta to update the shape of each surface and imposes incompressibility and contact interactions a posteriori.

The most important of this interactions pertains the free surface of the Earth which is taken to be impermeable and subject to stresses produced by the underlying lithosphere and mantle. A thin lubrication layer is interposed at the contact between the surface of the Earth and the plate (Morra et al., 2007; OzBench et al., 2008; Ribe, 2010) to reduce shear stresses in favour of normal ones, restoring isostatic equilibrium while letting the plates slide in any tangential direction and producing viscous bulging when bending. This mechanism allows the negative buoyancy of the lithosphere to induce realistic subduction instead of sinking. Interplate interactions are also affected by a lubrication layer that renders them frictionless. As plates converge, a minimum equilibrium distance between their surfaces is enforced by effectively deforming the overriding plates while maintaining the shape of the downgoing plate (Morra et al., 2012). A hierarchy of surfaces predefines which particular plates play the role of indentors relative to others.

Since the flow field is completely determined by the geometry of the interfaces, an expected global surface velocity field can be derived from plate morphology. Our geodynamic model is characterised by a high degree of *plateness* as plate deformations are localised at trenches, however, in order to compare with the rigid kinematic reconstructions, we calculate the Euler pole that best fits plate motion in a RMS sense. The location of the Euler pole, and consequently the direction of the velocity field is assumed to be more important than the actual magnitude of the motion since the latter can be fitted by careful selection of the viscosity contrast between mantle and lithosphere (Conrad and Lithgow-Bertelloni, 2004). Velocities are therefore renormalised to highlight their orientation.

3. Plate models from subduction history reconstruction

We produced models where slabs sink in the upper mantle with a radial (vertical) velocity equal to the convergence velocity normal to the trench, and models with a constant sinking rate. In both cases, we assume that the tangential (horizontal) motion of the subducted material follows the absolute Euler rotation of the subducting plate, and that the thickness of the plates is 90 km. This directly fixes the pull in the model according to the amount of material being subducted and produces a continuous slab with asymmetric suction.

To generate slabs (see Fig. 2) each point P in a convergent margin is displaced tangentially on the surface according to the velocity $\mathbf{v}_A$ of the point on the subducting plate A. This velocity is obtained by calculating the stage Euler pole ${}^{t_1}\mathbf{E}_A^{t_2}$ for the motion of the plate in the period $\Delta t = t_2 - t_1$ relative to the absolute frame of the reconstructions. Applying the associated rotation to each point in the trench one obtains the displacement $\Delta\mathbf{r}_A$ and therefore the velocity $\mathbf{v}_A = \Delta\mathbf{r}_A/\Delta t$. The sinking rate v_s is taken to be constant or calculated from the local convergence velocity $\mathbf{v}_{AB}$ of P which is derived from $\mathbf{v}_A$ and the velocity $\mathbf{v}_B$ of the point on the overriding plate B according to $\mathbf{v}_{AB} = \mathbf{v}_A - \mathbf{v}_B$. Projecting $\mathbf{v}_{AB}$ in a direction normal to the trench we obtain $\mathbf{v}_n$, the local convergence velocity normal to the trench. The combination of the tangential rotation and the radial sinking takes P to the point Q at the given time interval. In general, the local dip of the slab θ would be determined by the ratio of the sinking rate and the convergence velocity normal to the trench at the point, according to the expression

$$\theta = \tan^{-1}\left(\frac{v_s}{v_n}\right). \tag{2}$$

If we take the sinking speed to be precisely the convergence rate normal to the trench, then the dip is fixed to be 45°. Following this procedure, a trench that is static will not lead to a dip of 90° but one of 45° if the sinking speed corresponds to the convergence rate normal to the trench, and a steeper or shallower angle if the sinking speed exceeds or remains under this value, respectively.

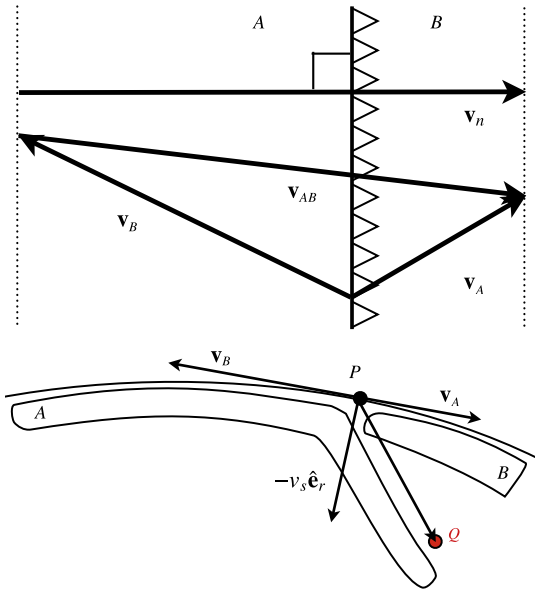

Fig. 2. Top: Map view of local velocity vectors $\mathbf{v}_A$ and $\mathbf{v}_B$ of the subducting (A) and overriding (B) plates, from which convergence rate is inferred by projecting $\mathbf{v}_{AB} = \mathbf{v}_A - \mathbf{v}_B$ normal to the trench ($\mathbf{v}_n$). Bottom: Section showing the tangential v_A and radial $-v_s$ velocity components of a point P that is to be displaced to Q on a given time interval.

Calculating the post-subduction history is done iteratively in 1 Myr time steps. At each step, position of material subducting at the marging is obtained from the Euler stage pole of the subducting plate, and sunk radially point by point according to a selected sinking speed.

4. Present day model results

Following the workflow described in Section 3, we have generated subduction history models of the 13 major plates at the present: Africa, Antarctica, Arabia, Australia, Caribbean, Cocos, Eurasia, Nazca, North America, Pacific, Philippines, Scotia and South America. The models are based on the kinematic reconstruction by Seton et al. (2012) and are extrapolated into the mantle taking into account the last 10 Myr of subduction history. Different setups were tested using a constant sinking rate of 5 cm/yr leading to variable slab dip in one case, and a 45° dip in the other.

We calculated the time evolution of the present day global models for viscosity contrasts between lithosphere and mantle ranging from 10 to 200 and with lower to upper mantle viscosity contrast ranging from 1 to 100. The system was let to evolve freely under the influence of gravity until a quasi-steady-state regime was achieved, in which plate motion was found to be relatively constant in time. The dips of the models approached 90° asymptotically, and the morphology of the slab profile became very similar regardless of the initial fixed or variable dip initial condition (see Fig. 3).

4.1. Modelled and observed velocities

We calculated the best fitting Euler pole associated with the motion of the nodes in the surface of each of the 13 plates after 1 Myr of evolution for the different parameters and initial dip angle, and found that the maximum angular distance between Euler poles of plates inferred from models with fixed and variable dip was of 6° for subducting plates and 15° for overriding ones.

We further calculated the average angular distance between the modelled and the reconstructed Euler poles during the last 1 Myr, based on the reconstruction of Seton et al. (2012) for 7 models of constant dip, and found that the Euler poles of subducting plates are better correlated to the reconstructions than non-subducting plates. The viscosity structure and the average angular misfit of the location of the poles for each model is described in Table 2.

Table 2
Viscosity structure of constant dip models and average angular misfit of Euler poles for subducting (S) and non-subducting (NS) plates.

Model	μ	μ_{LM}	S	NS
1	10	1	18°	28°
2	50	100	22°	23°
3	100	1	20°	27°
4	100	50	25°	24°
5	100	100	26°	26°
6	200	1	24°	32°
7	200	50	27°	29°

The poles are found in the mean mantle no net rotation reference frame in which they are calculated. The resulting net lithospheric rotation associated to the models varies between 0.001° Myr^{-1} and 0.03° Myr^{-1}.

Reducing the degree of mantle layering significantly increased the spread between subducting and non-subducting plates, whereas the models with homogeneous mantle consistently present better fits for subducting plates. The best overall fit weighting the plates by their total surface area, is obtained by model 3, shown in Fig. 4. The net lithospheric rotation for this case is of 0.03° Myr^{-1} around a pole at 68°S and 120°E.

As expected from a subduction-driven model, present day kinematics exhibits good match for subducting plate velocities (Pacific, Australia, Nazca, Cocos and Philippines) and a poor match for overriding plates (South America, North America, Africa, Arabia and the Caribbean), with the notable exception of Eurasia, which is not far off its observed rotation. The predicted motion of South America opposes the observed one, that of North America is oriented towards the Cocos slab and the Caribbean one is directed SE towards the small slab attached to South America.

5. 125 Ma model results

The 125 Ma model was derived through the same procedure as the present models, using the 10 Myr of tectonic evolution (from 135 Ma to 125 Ma) of the 10 major plates at the time: Africa, Eurasia, India, North America, Phoenix, East Gondwana, Farallon, Izanagi, Pacific and South America. Plate thickness was fixed at 90 km and only a fixed 45° dip was considered. Being completely surrounded by ridges, the Pacific plate was entirely removed from

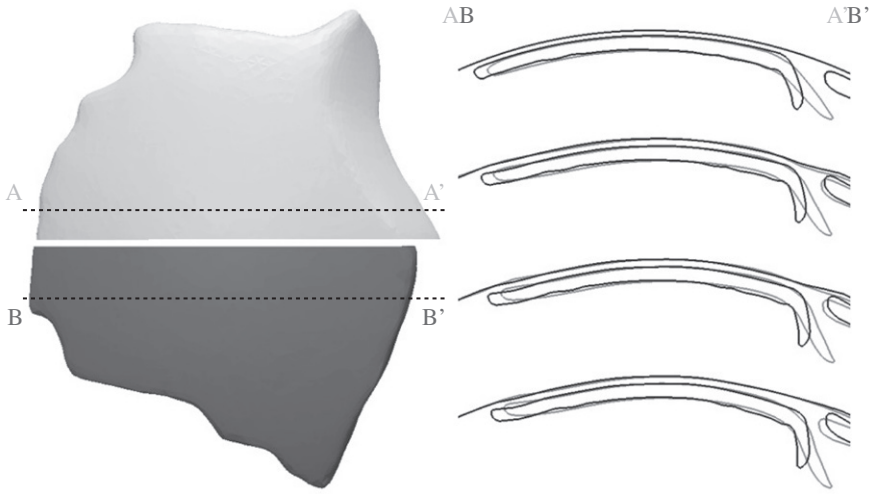

Fig. 3. Left: Top view of the initial condition for two models of the present day Nazca plate with a 45° dip (light grey) and constant sinking rate of 5 cm/yr (dark gray) and. Right: Cross sections showing the evolution of a simulation after 0, 100, 150 and 200 timesteps.

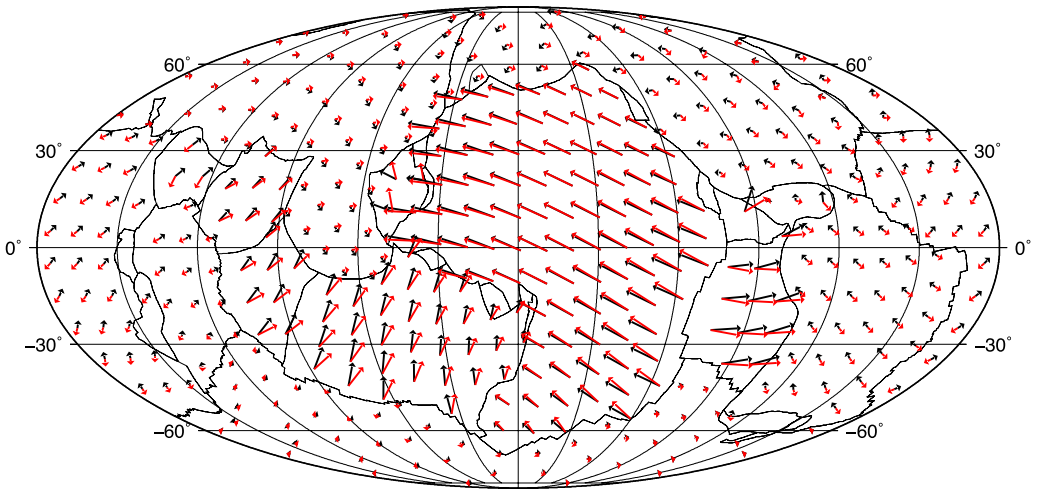

Fig. 4. Predicted (red) vs. observed (black) global kinematics for non-layered mantle (Model 3). (For interpretation of the references to colour in this figure legend, the reader is referred to the web version of this article.)

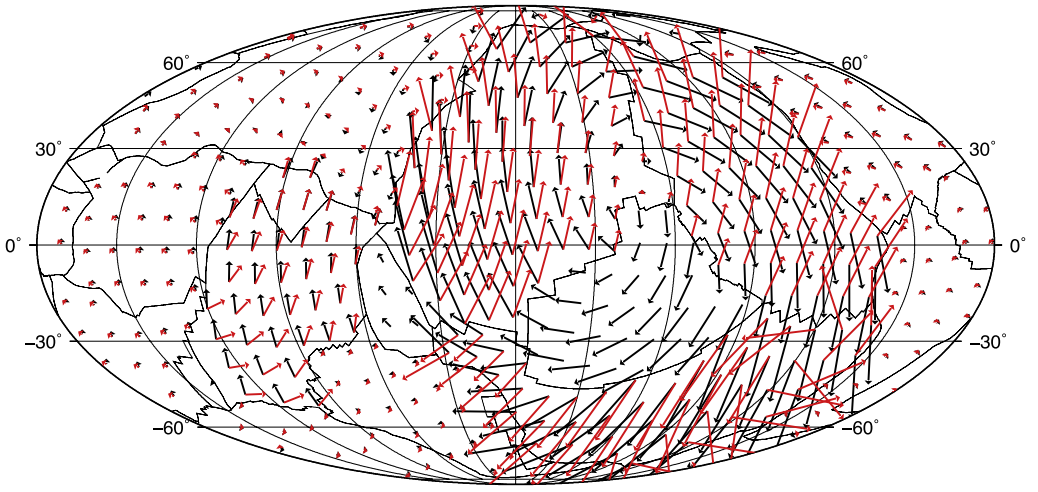

Fig. 5. Predicted (red) vs. reconstructed (black) global kinematics for non-layered mantle at 125 Ma. (For interpretation of the references to colour in this figure legend, the reader is referred to the web version of this article.)

the geodynamic models since its contribution to a top-down driven convective mantle flow is marginal.

In this case a single 1 Myr run with the same viscosity contrasts as model 3 above was performed, and analysed by abstracting the orientation of the motion through direct scaling of the magnitude of the velocities to the reconstructed values. The resulting global comparison of predicted vs. reconstructed is shown in Fig. 5.

The modelled absolute plate motions at 125 Ma show orientations that are generally well-correlated with the reconstruction, even for overriding plates. There is clear bias towards subduction zones as expected from a top down model. The India and Izanagi plates follow a symmetric and opposite rotation around their poles which might be evidence of interaction through mantle flow (Morra et al., 2012). However, the predicted kinematics of the Farallon plate is clearly at odds with the reconstructions, which are based on a combination of the hotspot track-based absolute plate motion by Wessel and Kroenke (2008) combined with a relative plate motion model described by Seton et al. (2012). This kinematic model results in transform motion along the western margin of North America, which is unlikely given that geological data suggest subduction at that time (DeCelles, 2004).

6. Discussion

6.1. Present day modelled and observed velocities

The modelled velocities are less sensitive to the initial dip than to their overall geometry in accordance with previous studies (Ribe, 2010; Morra et al., 2012). We were able to reproduce the general directions of motion of the subducting plates and to some extent the tendency of overriding plates to move towards subduction trenches. The velocity patterns result from the flow induced by the pull and suction of slabs in the upper mantle, that is, without tracing the slabs down to the lower mantle and without decoupling them from the plates to fit the balance between slab pull and slab suction (Conrad and Lithgow-Bertelloni, 2004). Previous analysis correlating the viscosity structure and the dynamics of plates (Lithgow-Bertelloni and Richards, 1998) suggest that the relative strength of the lithosphere has more effect on plate speed than on motion direction, whereas the upper/lower mantle heterogeneity has more effect on the directions than on speed. Our results suggests that by tuning the mantle viscosity structure, the self-consistent pull and suction induced by coherent slabs could

alone lead to a good fit with observed plate kinematics, regardless of the particular mantle flow control of the interactions responsible for the alterations of the balance of plate driving forces. This is also consistent with the conclusions of a parameter space study included in Morra et al. (2012), where a homogeneous mantle was shown to result in increased plateness and plate behaviour mainly controlled by pull.

The slight convergence between South America and Africa (both non-subducting plates) is caused by the intraplate interaction induced by the Nazca plate acting as an indentor to South America, which is then viscously deformed. This deformation reduces plateness and introduces additional uncertainties in the determination of the best fitting Euler pole for this plate. The deviation of the Australian rotation pole with respect to the observed one is explained by the bias towards the New Hebrides–Fiji and Tonga–Kermadec subduction zones. On the other hand, the motion of the African and Arabic plates does not correspond well with the observed absolute motions due to the absence of a slab corresponding to the Tethys subduction in our model (which considers only the last 10 Myr of history). Considering a longer period of subduction to generate a better model may alleviate these mismatches.

It is known that radial mantle viscosity layering reduces the sinking velocity of the plate (Morra et al., 2010), when modelling its dynamic behaviour from first principles. This suggests that a simple improvement of our slab position estimation could be achieved by introducing a radially weighted sinking velocity profile in a similar fashion as in (Lithgow-Bertelloni and Richards, 1998, Fig. 5), to represent how flow crossing layers of increased viscosity and density is retarded without explicitly modelling by studying its dynamics. Such approximation might lead to a reasonable estimate for the amount of material accumulating on top of the 660 km boundary, allow a more realistic description of dynamical properties and fields like the geoid, and may be useful in the study of true polar wander as a consequence of the time-dependence of plate motions and subduction.

Considering varying continental lithospheric thickness has a marginal effect on subduction dynamics (Butterworth et al., 2012) and is more relevant to small scale convection in the upper mantle (King and Ritsema, 2000) than to the global pattern of flow. Nevertheless its implementation is particularly simple and does not increase computational complexity. The surface mesh tailored for FastBEM applications may be rendered into full 3D volumetric models by applying smoothing density/viscosity factors around them as done in (Stadler et al., 2010, Section 2.2). Additional information like changes in material properties in the transition from continental to oceanic lithosphere can be inferred from the geological features of reconstructions and assigned as attributes to the points using the continuously closing plate polygons algorithm (Gurnis et al., 2012) implemented on GPlates. Initial boundary conditions for finite-element-based geodynamic modelling software like CitcomS or Terra can be generated in this way.

6.2. 125 Ma modelled and reconstructed velocities

The most remarkable result is that considering the worst misfit inferred from the present day models, the predicted motion of the Farallon plate in the 125 Ma model is more consistent with the history of subduction inferred from regional geology (DeCelles, 2004) than with plate kinematic reconstructions at the particular time. This is particularly significant given the negligible difference between the modelled and reconstructed motion of North America.

Plate kinematic models against which we compare our results are subject to great uncertainties, particularly in the determination of absolute motions. There is very little data to constrain absolute plate motions of the Pacific Plate for the period from 120 to 140 Ma. This concerns both a paucity of hotspot tracks as well as age dates. The absolute plate motion model with which we compare our dynamic model during this period, mainly depends on the current knowledge of the geometry and age of the Mid-Pacific Mountains and the Shatsky Rise (Wessel and Kroenke, 2008). Even if we were to obtain more detailed maps and more precise isotope age dates for these features, sparse data from a small Early Cretaceous part of the Pacific Plate would be insufficient to determine absolute plate motions for the plates in the ocean basin surrounding it. Yet at 125 Ma, the qualitative agreement between the reconstructed and the predicted motion of Izanagi and Phoenix away from ridges and towards subduction zones strengthens our confidence in these features of the reconstruction; in contrast, the discrepancy between kinematics and simulated dynamics in the case of the Farallon plate weakens it. A similar reasoning applied to the Farallon plate motion as described by the reconstruction of Torsvik et al. (2010), which is based on the absolute plate motion model of Duncan and Hague (1985) leads to a better fit.

For similar cases where the mismatch of the predicted and reconstructed absolute motions is specially important in a region where the errors are big and observations scarce, geodynamic models based on subduction history seem to be unique in helping constrain plate kinematics. In a more general context, the fact that the expected kinematic convergence behaviour, considering geological observations, can be inferred from the *history* of subduction even when the particular kinematic model at the time is at odds with it, is an indication that our slab history model is very robust and less sensitive to short term transient regimes. Such robustness opens the possibility of assessing the consistency of kinematic reconstructions, and would provide a tool to revise reconstruction models by locating where and when reconstructed kinematics is inconsistent with the dynamics expected from plate geometry and subduction history.

7. Conclusions

We show that a subduction history model based on the advection of slab material into the mantle following reconstructed kinematic constraints captures the main dynamic features of upper mantle heterogeneities.

The modelled mantle structure represents an average behaviour integrated over time that is robust and stable against transient regimes and local regional variations. These attributes make these models suitable as initial conditions for geodynamic simulation codes that assume a relatively simple compositional and rheological complexity. This is particularly important when inferring dynamic properties associated to a particular plate tectonic reconstruction, since it allows to isolate the effect of a smaller number of physical parameters. The workflow developed is tailored for Boundary Element based applications like BEMEarth where the input is parametrized by 3D surface data, however, volume 3D meshes for Finite Element Method based geodynamic software like CitcomS (Zhong et al., 2000; Tan et al., 2006) or Terra (Bunge and Baumgardner, 1995) would be easy to build.

Kinematically constrained simulations would benefit from a simpler initial guess for the mantle structure which would translate into significant increase in speed up and accuracy, specially by avoiding dealing with complex compositional variations at lithospheric depth. It also opens the door to data assimilation from a paleo-model instead of present day data that could push the analysis further back in time. For self-consistent simulations, the workflow developed could provide a computationally efficient way to compare and contrast kinematic reconstructions. In the Cenozoic and present day by directly matching with tomographical and geodetic observations, and in general, by analysing the correlations between observed and predicted dynamic properties like

plate motions, the associated dynamic topography, and potentially the geoid.

This workflow is useful as a straightforward quality metric for different reconstructions based on their dynamic properties and could be used to improve absolute plate reconstruction models and reference frames (Shephard et al., 2012; van der Meer et al., 2010), by improving their consistency with their associated dynamical effects. The prediction of subducting plate motion orientation and the reproduction of the tendency of overriding plates to move towards trenches following the influence of suction and ridge push, and using a homogeneous mantle, leaves enough freedom in the parameter space of the simulations to fit reconstructed plate kinematics precisely.

Acknowledgements

The authors would like to thank the Australian Research Council for financial support (DP0986377). G.M. thanks the Swiss National Science Foundation (Advanced Researcher Fellowship PA0022-121475) and the Korean government (MEST, No. 2009-0092790) for financial support. R.D.M. thanks the Australian Research Council for financial support (Laureate Fellowship). We thank F. Capitanio and an anonymous reviewer for their constructive comments; and T. Landgrebe, C. Heine, M. Seton, N. Flament, G. Shepherd, N. Butterworth and A. Talsma for fruitful discussions. Maps were generated with the Generic Mapping Tools (Wessel and Smith, 1991).

Appendix A. Surface mesh generation

Subduction history reconstruction is estimated from data sampled with user controlled resolution resulting in a set of points with low noise and high degree of regularity. This suggests the direct use of α-shape sculpting methods (Bernardini and Bajaj, 1997; Edelsbrunner and Mücke, 1992; Edelsbrunner et al., 1983) above other techniques as the implicit function (Kazhdan et al., 2006; Hoppe et al., 1992), Moving Least Squares (Alexa et al., 2003), Delaunay-based (Boissonnat, 1984; Amenta and Bern, 1999) and ball-pivoting (Bernardini et al., 2002) methods, to produce the triangulated surface mesh defining the viscosity contrast layer that describes the lithosphere in our models. α-Shapes are one of the simplest constructions that provide a clear definition of the "shape" formed by an unorganised set of points. The frontier of an α-shape is a linear approximation of the original shape that is constructed by carving the space around and between points by balls of radius α (see Fig. A1). A simple intuitive description may be given in the form of a chocolate chip ice cream: Scooping the ice without taking any chocolate chips will essentially result in an α-shape, where α is the radius of the scoop (carving holes on the inside is allowed). The resulting shape is not necessarily convex or simply connected. Changing α has an effect on the topology of the resulting object: for α smaller than the smallest inter-particle distance we recover the original point cloud, whereas in the limit $\alpha \to \infty$ we obtain its convex hull. We tune α until we find the shape that produces a single tectonic plate out of the points surrounding its geometry.

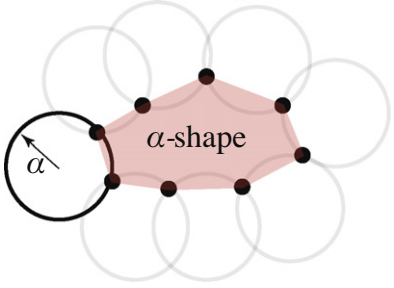

Fig. A1. α-Shape construction.

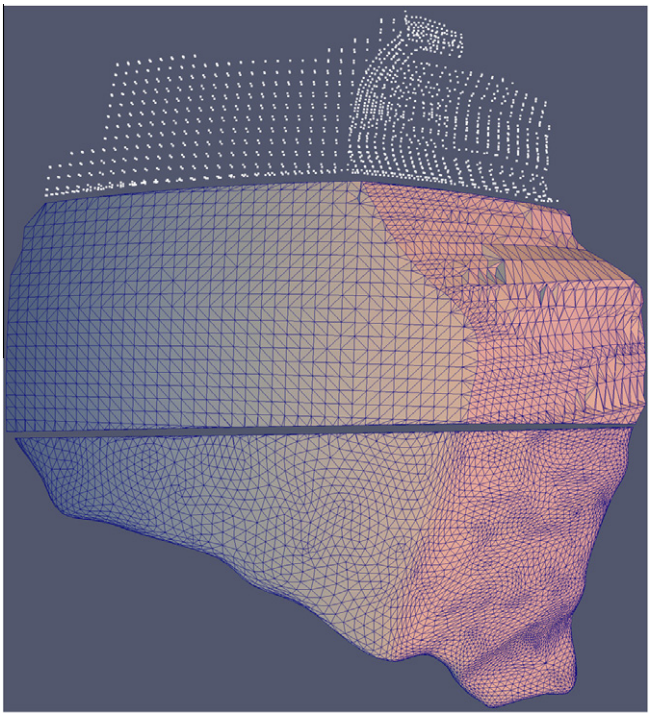

Fig. A2. Three different stages of mesh generation for the present-day Nazca plate. Top: original point cloud from subduction history reconstruction. Middle: initial α-shape. Bottom: smooth surface mesh.

The resulting mesh is optimised for finite or boundary element methods by cutting out overlappings, smoothing, and subdividing(simplifying) up(down) to a particular number of elements. We have found that the strategy of alternating subdivision and simplification algorithms is a fast and robust substitute to more involved remeshing, and handles well the appearance of vertices with excessive number of edges (see Fig. A2). The mesh generation and processing steps were implemented using the Computational Geometry Algorithms Library (CGAL) which provides Nef polyhedra operations, α-shape generation, surface simplification and subdivision algorithms (Granados et al., 2003; Garland and Heckbert, 1997; Shiue, 2005).

References

Alexa, M., Behr, J., Cohen-Or, D., Fleishman, S., Levin, D., Silva, C., 2003. Computing and rendering point set surfaces. IEEE Transactions on Visualization and Computer Graphics, pp. 3–15.

Amenta, N., Bern, M., 1999. Surface reconstruction by Voronoi filtering. Discrete and Computational Geometry 22, 481–504.

Anderson, D.L., 1982. Hotspots, polar wander, mesozoic convection and the geoid. Nature 297, 391–393.

Becker, T., 2010. Fine-scale modeling of global plate tectonics. Science 329, 1020–1021.

Bellahsen, N., Faccenna, C., Funiciello, F., 2005. Dynamics of subduction and plate motion in laboratory experiments: insights into the plate tectonics behavior of the Earth. Journal of Geophysical Research 110, B01401.

Bernardini, F., Bajaj, C., 1997. Sampling and reconstructing manifolds using alpha-shapes. In: Proceedings of 9th Canadian Conference Computational Geometry, pp. 193–198.

Bernardini, F., Mittleman, J., Rushmeier, H., Silva, C., Taubin, G., 2002. The ball-pivoting algorithm for surface reconstruction. IEEE Transactions on Visualization and Computer Graphics 5, 349–359.

Billen, M., 2008. Modeling the dynamics of subducting slabs. Annual Review of Earth and Planetary Sciences 36, 325.

Boissonnat, J., 1984. Geometric structures for three-dimensional shape representation. ACM Transactions on Graphics (TOG) 3, 266–286.

Bunge, H.P., Baumgardner, J.R., 1995. Mantle convection modeling on parallel virtual machines. Computers in Physics 9, 207–215.
Bunge, H.P., Hagelberg, C.R., Travis, B.J., 2003. Mantle circulation models with variational data assimilation: inferring past mantle flow and structure from plate motion histories and seismic tomography. Geophysical Journal International 152, 280–301.
Bunge, H.P., Richards, M.A., Lithgow-Bertelloni, C., Baumgardner, J.R., Grand, S.P., Romanowicz, B.A., 1998. Time scales and heterogeneous structure in geodynamic Earth models. Science 280, 91–95.
Butterworth, N.P., Quevedo, L., Morra, G., Müller, R.D., 2012. Influence of overriding plate geometry and rheology on subduction. Geochemistry, Geophysics, and Geosystems 13, Q06W15.
Capitanio, F., Faccenna, C., Zlotnik, S., Stegman, D., 2011. Subduction dynamics and the origin of Andean orogeny and the Bolivian orocline. Nature 480, 83–86.
Capitanio, F.A., Morra, G., Goes, S., 2007. Dynamic models of downgoing plate-buoyancy driven subduction: subduction motions and energy dissipation. Earth and Planetary Science Letters 262, 284–297.
Capitanio, F.A., Morra, G., Goes, S., 2009. Dynamics of plate bending at the trench and slab-plate coupling. Geochemistry, Geophysics and Geosystems 10, Q04002.
Chase, C.G., 1979. Subduction, the geoid, and lower mantle convection. Nature 282, 464–468.
Chase, C.G., Sprowl, D.R., 1983. The modern geoid and ancient plate boundaries. Earth and Planetary Science Letters 62, 314–320.
Cloos, M., 1993. Lithospheric buoyancy and collisional orogenesis: Subduction of oceanic plateaus, continental margins, island arcs, spreading ridges, and seamounts. Geological Society of America Bulletin 105, 715–737.
Conrad, C.P., Lithgow-Bertelloni, C., 2002. How mantle slabs drive plate tectonics. Science 298, 207–209.
Conrad, C.P., Lithgow-Bertelloni, C., 2004. The temporal evolution of plate driving forces: importance of slab suction versus slab pull during the Cenozoic. Journal of Geophysical Research 109, B10407.
DeCelles, P., 2004. Late Jurassic to Eocene evolution of the Cordilleran thrust belt and foreland basin system, western USA. American Journal of Science 304, 105.
Duncan, R., Hague, D., 1985. Pacific plate motion recorded by linear volcanic chains. Ocean Basins and Margins 7, 89.
Edelsbrunner, H., Kirkpatrick, D., Seidel, R., 1983. On the shape of a set of points in the plane. IEEE Transactions on Information Theory 29, 551–559.
Edelsbrunner, H., Mücke, E., 1992. Three-dimensional alpha shapes. In: Proceedings of the 1992 Workshop on Volume Visualization, ACM, pp. 75–82.
Forsyth, D., Uyeda, S., 1975. On the relative importance of the driving forces of plate motion. Geophysical Journal of the Royal Astronomical Society 43, 163–200.
Funiciello, F., Morra, G., Regenauer-Lieb, K., Giardini, D., 2003. Dynamics of retreating slabs. 1: insights from two-dimensional numerical experiments. Journal of Geophysical Research-Solid Earth 108, 2206.
Garland, M., Heckbert, P., 1997. Surface simplification using quadric error metrics. In: Proceedings of the 24th Annual Conference on Computer Graphics and Interactive Techniques, ACM Press/Addison-Wesley Publishing Co. pp. 209–216.
Gerya, T., Connolly, J., Yuen, D., 2008. Why is terrestrial subduction one-sided? Geology 36, 43.
Granados, M., Hachenberger, P., Hert, S., Kettner, L., Mehlhorn, K., Seel, M., 2003. Boolean operations on 3d selective nef complexes: data structure, algorithms, and implementation. Algorithms-ESA 2003, 654–666.
Gurnis, M., 1993. Phanerozoic marine inundation of continents driven by dynamic topography above subducting slabs. Nature 364, 589–593.
Gurnis, M., Turner, M., Zahirovic, S., DiCaprio, L., Spasojevic, S., Müller, R.D., Boyden, J., Seton, M., Manea, V.C., Bower, D.J., 2012. Plate tectonic reconstructions with continuously closing plates. Computers and Geosciences 38, 35–42.
Hoppe, H., DeRose, T., Duchamp, T., McDonald, J., Stuetzle, W., 1992. Surface reconstruction from unorganized points. SIGGRAPH Computer Graphics 26, 71–78.
Iaffaldano, G., Bunge, H., Dixon, T., 2006. Feedback between mountain belt growth and plate convergence. Geology 34, 893.
Kazhdan, M., Bolitho, M., Hoppe, H., 2006. Poisson surface reconstruction. In: Proceedings of the Fourth Eurographics Symposium on Geometry Processing, Eurographics Association. pp. 61–70.
King, S.D., Ritsema, J., 2000. African hot spot volcanism: small-scale convection in the upper mantle beneath cratons. Science 290, 1137–1140.
Lithgow-Bertelloni, C., Gurnis, M., 1997. Cenozoic subsidence and uplift of continents from time-varying dynamic topography. Geology 25, 735–738.
Lithgow-Bertelloni, C., Richards, M.A., 1995. Cenozoic plate driving forces. Geophysical Research Letters 22, 1317–1320.
Lithgow-Bertelloni, C., Richards, M.A., 1998. The dynamics of cenozoic and mesozoic plate motions. Reviews of Geophysics 36, 27–78.
van der Meer, D.G., Spakman, W., van Hinsbergen, D.J.J., Amaru, M.L., Torsvik, T.H., 2010. Towards absolute plate motions constrained by lower-mantle slab remnants. Nature Geoscience 3, 36–40.
Mitrovica, J., 1996. Haskell [1935] revisited. Journal of Geophysical Research 101, 555–569.
Morra, G., Chatelain, P., Tackley, P., Koumoutsakos, P., 2007. Large scale three-dimensional boundary element simulation of subduction. In: Shi, Y., van Albada, G.D., Dongarra, J., Sloot, P.M. (Eds.), Computational Science – ICCS 2007 7th International Conference, Beijing, China, May 27–30, 2007. Proceedings, Part III, Springer. pp. 1122–1129.
Morra, G., Chatelain, P., Tackley, P., Koumoutsakos, P., 2009. Earth curvature effects on subduction morphology: modeling subduction in a spherical setting. Acta Geotechnica 4, 95–105.
Morra, G., Quevedo, L., Müller, R.D., 2012. Spherical dynamic models of top-down tectonics. Geochemistry, Geophysics and Geosystems 13, Q03005.
Morra, G., Yuen, D.A., Boschi, L., Chatelain, P., Koumoutsakos, P., Tackley, P.J., 2010. The fate of the slabs interacting with a density/viscosity hill in the mid-mantle. Physics of the Earth and Planetary Interiors 180, 271–282.
OzBench, M., Regenauer-Lieb, K., Stegman, D.R., Morra, G., Farrington, R., Hale, A., May, D.A., Freeman, J., Bourgouin, L., Mühlhaus, H., Moresi, L., 2008. A model comparison study of large-scale mantle–lithosphere dynamics driven by subduction. Physics of the Earth and Planetary Interiors 171, 224–234.
Pozrikidis, C., 1992. Boundary Integral and Singularity Methods for Linearized Viscous Flow, vol. 7. Cambridge University Press, Cambridge.
Quevedo, L., Hansra, B., Morra, G., Butterworth, N., Müller, R.D., 2012. Oblique mid ocean ridge subduction modelling with the parallel fast multipole boundary element method. Computational Mechanics, 1–9.
Quevedo, L., Morra, G., Müller, R.D., 2010. Parallel fast multipole boundary element method for crustal dynamics. IOP Conference Series: Materials Science and Engineering 10, 012012.
Ribe, N., 2010. Bending mechanics and mode selection in free subduction: a thin-sheet analysis. Geophysical Journal International 180, 559–576.
Ricard, Y., Richards, M., Lithgow-Bertelloni, C., LeStunff, Y., 1993. A geodynamic model of mantle density heterogeneity. Journal of Geophysical Research 98, 21895–21909.
Richards, M.A., Engebretson, D.C., 1992. Large-scale mantle convection and the history of subduction. Nature 355, 437–440.
Schellart, W., 2005. Influence of the subducting plate velocity on the geometry of the slab and migration of the subduction hinge. Earth and Planetary Science Letters 231, 197–219.
Seton, M., Müller, R.D., Zahirovic, S., Gaina, C., Torsvik, T., Shephard, G., Talsma, A., Gurnis, M., Turner, M., Maus, S., Chandler, M., 2012. Global continental and ocean basin reconstructions since 200 Ma. Earth-Science Reviews 113, 212–270.
Shephard, G., Bunge, H.P., Schuberth, B., Müller, R., Talsma, A., Moder, C., Landgrebe, T., 2012. Testing absolute plate reference frames and the implications for the generation of geodynamic mantle heterogeneity structure. Earth and Planetary Science Letters 317–318, 204–217.
Shiue, L., 2005. Mesh refinement based on Euler encoding. In: Shape Modeling and Applications, 2005 International Conference, IEEE. pp. 343–348.
Stadler, G., Gurnis, M., Burstedde, C., Wilcox, L.C., Alisic, L., Ghattas, O., 2010. The dynamics of plate tectonics and mantle flow: from local to global scales. Science 329, 1033–1038.
Stegman, D.R., Freeman, J., Schellart, W.P., Moresi, L., May, D., 2006. Influence of trench width on subduction hinge retreat rates in 3-D models of slab rollback. Geochemistry, Geophysics and Geosystems 7, Q03012.
Steinberger, B., 2000. Slabs in the lower mantle – results of dynamic modelling compared with tomographic images and the geoid. Physics of the Earth and Planetary Interiors 118, 241–257.
Steinberger, B., Torsvik, T., 2010. Toward an explanation for the present and past locations of the poles. Geochemistry, Geophysics, and Geosystems 11, Q06W06.
Tan, E., Choi, E., Thoutireddy, P., Gurnis, M., Aivazis, M., 2006. GeoFramework: coupling multiple models of mantle convection within a computational framework. Geochemistry Geophysics and Geosystems 7, Q06001.
Torsvik, T.H., Steinberger, B., Gurnis, M., Gaina, C., 2010. Plate tectonics and net lithosphere rotation over the past 150 my. Earth and Planetary Science Letters 291, 106–112.
Wessel, P., Kroenke, L.W., 2008. Pacific absolute plate motion since 145 Ma: an assessment of the fixed hot spot hypothesis. Journal of Geophysical Research 113, B06101.
Wessel, P., Smith, W., 1991. Free software helps map and display data. EOS Transactions 72, 441.
Zhong, S., Zuber, M.T., Moresi, L., Gurnis, M., 2000. Role of temperature-dependent viscosity and surface plates in spherical shell models of mantle convection. Journal of Geophysical Research 105, 11063–11082.